# Investigations of the Chemical Bonding in the $P_4O_6S_m$ ($m = 0-4$) Series by Combination of Experimental and Theoretical Vibrational Analysis

**A. R. S. Valentim, B. Engels,* and S. D. Peyerimhoff**

*Institut für Physikalische und Theoretische Chemie, Universität Bonn, Wegelerstrasse 12, 53115 Bonn, Germany*

*Received: November 6, 1998; In Final Form: April 26, 1999*

The bonding situation within the $P_4O_6S_m$ ($m = 0-4$) series is studied using a combination of experimental and theoretical vibrational analysis. A correlation between the spectra of the compounds is undertaken and the shifts of the vibrational frequencies within the series are analyzed. The frequency shifts found within the $P_4O_6S_m$ ($m = 0-4$) series are furthermore compared with those found within the $P_4O_n$ ($n = 6-10$) series. Our analysis indicates a somewhat larger increases in the P−O cage bond strength in the oxygen-substituted compounds relative to the sulfur substitution. This interpretation is consistent with the same conclusion based on a comparison of the P−O bond lengths shortening in the cage in going from $P_4O_6$ to $P_4O_{10}$ (0.05 Å) and $P_4O_6$ to $P_4O_6S_4$ (0.03 Å).

## Section 1. Introduction

Phosphorchalcogenides, $P_4O_6X_n$ (X = O, S, Se; $n = 0-4$), which have been studied extensively in recent years,[1] form a specially tailored system. The gradual changes observed in their bonding properties along the series make them an ideal system for an investigation of the relationship between the molecular geometry and the strength of chemical bonding. Since the force field of a molecule is directly related to its bonding situation, a detailed analysis of the vibrational spectrum provides the possibility to study the strength of its chemical bonds. In previous work,[2−4] we used this approach to study the influence of the substituents X on the $P_4O_6$ cage bonds.

Employing ab initio methods, we computed the IR and Raman vibrational frequencies to assign the experimental spectra. Using the scaled quantum mechanics (SQM) method proposed by Pulay,[5] the theoretical and the experimental data were combined to obtain improved theoretical force fields. Since only the theoretical data allow an reliable correlation of the vibrational bands from one spectrum to another within the series, this combined approach used for vibrational analysis made it possible to study quantitatively the variations in the force field of the $P_4O_6X$ molecules.

In previous works,[2,3] differences in the cage bonds situation in the monosubstituted and disubstituted series, $P_4O_6X_m$ (X = O, S, Se; $m = 1-2$), have been studied by analyzing the frequency shifts in their vibrational spectra. In addition, the variations in the vibrational spectra connected with the $P^V = X$ (X = O, S, and Se) terminal bond were analyzed. These changes are less interesting, because they reflect the known relation between the different masses and bond strengths of the $P^V = X$ bond. Nevertheless, they must be considered because of their couplings to cage vibrations.

In our recent investigation,[4] the variations of the bonding situation within the series $P_4O_n$ ($n = 6-10$) have been studied. The results showed that vibrations, which involve motions of the oxygen substituents (relative to the cage), appear either in the low-energy region or in the high-energy region of the vibrational spectrum. In the energy range above 1100 $cm^{-1}$, only *stretching* vibrations of the terminal P═O bonds are observed. These bonds are so strong that couplings of the P═O stretching motions with motions of the P−O cage bonds are small. In the low-energy range (below 260 $cm^{-1}$), all bands correspond to bending motions of the terminal P═O bonds. These vibrations couple with libration of the $P_4O_6$ cage. The band shift to higher frequencies within the $P_4O_n$ ($n = 6-10$) series, which is observed in the middle range of the spectrum (300−1000 $cm^{-1}$), is a clear indication for the increase in the strength of the P−O cage bonds. Only for two bands, a shift to lower frequencies occurs, but this effect results from the increase of the mass of the moving units when going from $P_4O_6$ (phosphorus atom) to $P_4O_{10}$ (P═O unit).

In the present work, the vibrational spectra of the $P_4O_6S_m$ ($m = 0-4$) series will be studied. Differences between this series and the oxygen series $P_4O_n$ ($n = 6-10$) will be discussed to analyze if oxygen influences the $P_4O_6$ cage bonds stronger than sulfur substituents. This question is still under debate since the difference in the cage bond contraction in the two series is very small (≈2 pm).

Experimental IR and Raman spectra are already known for $P_4O_6S_m$ ($m = 1-4$).[2,3,6−8] The spectra of $P_4O_6S$ and $P_4O_6S_2$ have been already assigned employing ab initio methods, while for $P_4O_6S_4$ only a preliminary experimental assignment based on the Raman polarization measurements is known.[8] For $P_4O_6S_3$, no assignment has been reported so far.

## Section 2. Technical Details

The theoretical methods used in the present work are already discussed in our previous works.[2−4] Molecular equilibrium geometries were optimized employing the SCF method in combination with a DZP basis set given by Huzinaga,[9] and the vibrational frequencies and IR and Raman intensities were calculated at the stationary point of the molecules under consideration. All these calculations were performed with the Gaussian94 program package.[10] Errors of the HF force field

* To whom correspondence should be addressed. E-mail: bernd@thch.uni-bonn.de. Fax: (0228) 73-9066.

10.1021/jp984338f CCC: $18.00 
Published on Web 07/16/1999

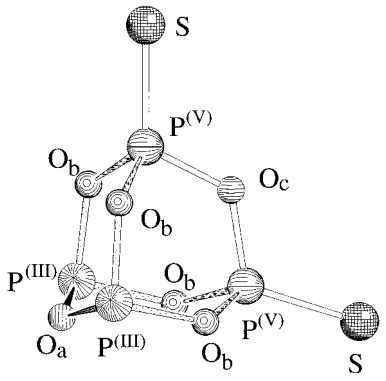


**Figure 1.** Molecular Structure of $P_4O_6S_2$; schematic illustration of the different P−O bonds. The four different bonds (within $C_{2v}$ symmetry) are specified by different shadings.

were corrected with the scaled quantum mechanical (SQM)[11] force field as proposed by Pulay and co-workers.[5]

Scale factors were obtained by a least-squares fit to known experimental data of $P_4O_6$, $P_4O_6S$, and $P_4O_6S_4$. Because the scaled frequencies of the present work were obtained employing averaged scaling factors, a small deviation ($\approx$10 cm$^{-1}$) exists to previous theoretical data, where individually optimized scaling factors were used. Descriptions of the nuclear displacements in the various modes were obtained using animations of the program MOLDEN.[12]

### Section 3. Results and Discussion

The molecular structure of $P_4O_6S_2$ together with a summary of abbreviation used in the present paper is given in Figure 1.

A comparison between the experimental and the theoretical bond distances (Table 1) shows that the geometrical parameter optimized at the HF/DZP level generally deviate by less than 1.5 pm from those obtained by X-ray diffraction methods.[6] As already described earlier,[1] substitution of the $P_4O_6$ cage by chalcogenide leads to a shortening of the bonds between $P^V$ and the neighboring oxygens ($O_b$) and an elongation of the $O_b-P^{III}$ bonds.

In $P_4O_6S_4$, the P−O cage bonds are 162 pm; i.e., they are shorter by about 3 pm than those in $P_4O_6$ (165 pm). This constitutes a smaller contraction of the P−O cage bonds due to the sulfur addition than found in the equivalent $P_4O_n$ ($n = 6-10$) series due to oxygen addition, where the cage bonds are 160 pm in $P_4O_{10}$. This bond difference between $P_4O_{10}$ and $P_4O_6S_4$ is too small to make the definitive statement that oxygen or sulfur substituents have a different influence on these cage bonds. On the other hand, a finding that the frequency shifts along the $P_4O_6S_m$ ($m = 0-4$) series are smaller than those observed for the oxygen substitution could support such a conclusion based on the cage bond length contraction.

**Theoretical and Experimental Frequencies.** The vibrational frequencies of the $P_4O_6S_m$ ($m = 0-4$) molecules obtained from various measurements and calculations are collected in Tables 2−6. The calculated vibrational frequencies for $P_4O_6$, which have been already reported in our previous study,[4] are also listed in Table 6 for comparison. The accuracy of the data are similar to those found for the $P_4O_n$ ($n = 6-10$) series,[4] i.e., in the range of 10 cm$^{-1}$.

In the following the IR and Raman spectra of $P_4O_6S_m$ ($m = 3-4$) will be assigned. The assignment for the $P_4O_6S$ and $P_4O_6S_2$ can be taken from our earlier work.[2−4] As observed for $P_4O_6S$ and $P_4O_6S_2$, the bending modes of the $P^V$═S units are found in the lower region of the spectrum of $P_4O_6S_3$: the two lowest modes (Table 4) correspond to a linear combination of the motion of the $P^V$═S units (1e: 148 cm$^{-1}$; $1a_1$: 160 cm$^{-1}$). Both modes possess strong Raman intensities but very small IR intensities. The strongest band in the Raman spectra of $P_4O_6S_3$ corresponds to the cage breathing mode, which is experimentally found at 485 cm$^{-1}$ (theoretical 479 cm$^{-1}$). The $P^V$═S *stretching* vibrations of $P_4O_6S_3$ are the $7a_1$ mode (891 cm$^{-1}$) and the 10e mode (795 cm$^{-1}$). The highest two modes (11e, $8a_1$) in the spectrum of $P_4O_6S_3$ correspond to stretching vibrations within the $PO_3$ units of the $P_4O_6$ cage. They are computed at 974 and 970 cm$^{-1}$, respectively, and are observed in the infrared spectrum as a very strong and broad band at 960 cm$^{-1}$.

Table 5 gives a comparison between our computed frequencies of $P_4O_6S_4$ and experimental results taken from the literature. The agreement between our data and those given by Jansen and co-workers is good,[1,6] taking into account that crystal environment effects lead to a lower symmetry and, hence, to a splitting of degenerate modes. Additional bands in the experimental spectra may be attributed to combination bands or overtones. An example is the band found at 387 cm$^{-1}$. This band does not fit to any computed fundamental, but may arise from a combination band of the lowest $f_2$ mode (158 cm$^{-1}$) and the lowest $f_1$ mode (220 cm$^{-1}$). Bands in this experimental spectra which appear above 1100 cm$^{-1}$ must stem from residuary oxygen compounds, as was already assumed by Clade et al.[1]

For $P_4O_6S_4$, the $P^V$═S stretch modes are localized in the same energy range as the stretching vibrations of the P−O cage bonds ($\approx$900 cm$^{-1}$). The in-phase motion of the $P^V$═S is found at 929 cm$^{-1}$, while the out-of-phase motion is located at 807 cm$^{-1}$ ($5f_2$). The highest mode in the $P_4O_6S_4$ spectrum is the $6f_2$ mode (986 cm$^{-1}$). While the $5f_2$ corresponds mainly to an out-of-phase stretching motion of the $P^V$═S, with a small contribution of the cage modes, the $6f_2$ can be described as a symmetric stretching motion of the P−O cage bonds with a small contribution of the $P^V$═S stretching. The coupling of $P^V$═S and the P−O cage vibrations indicate that the products of their respective **G** und **F** matrix elements are similar.

**Comparison of the Vibrational Spectra of $P_4O_6S_m$ ($m = 0-4$) Series.** Our comparison of the vibrational spectra of the molecules $P_4O_6S_m$ ($m = 0-4$) is based on the computed frequencies, obtained with the SQM force field technique. Discussing the vibrations in terms of linear combinations of

**TABLE 1: Bond Lengths (in Å) in Phosphorus Oxide Sulfide[a]**

| | $P_4O_6$ | | $P_4O_6S$ | | $P_4O_6S_2$ | | $P_4O_6S_3$ | | $P_4O_6S_4$ | |
|---|---|---|---|---|---|---|---|---|---|---|
| bonds | exptl | theor | exptl | theor | exptl | theor | exptl | theor | exptl | theor |
| $P^{(III)}-O_a$ | 1.653 | 1.648 | 1.637 | 1.646 | 1.636 | 1.645 | | | | |
| $P^{(III)}-O_b$ | | | 1.678 | 1.662 | 1.671 | 1.659 | 1.661 | 1.657 | | |
| $P^{(V)}-O_b$ | | | 1.596 | 1.611 | 1.595 | 1.611 | 1.595 | 1.613 | | |
| $P^{(V)}-O_c$ | | | | | 1.614 | 1.624 | 1.611 | 1.625 | 1.620 | 1.624 |
| $P^{(V)}-S$ | | | 1.890 | 1.882 | 1.885 | 1.876 | 1.882 | 1.868 | 1.886 | 1.864 |

[a] All theoretical values are obtained from a HF/DZP geometry optimization,[3,13] while the experimental data are X-ray data given in a review by Clade et al.[1]

**TABLE 2: Comparison of the Calculated Vibrational Spectra of $P_4O_6S$ with Experimental Data (in $cm^{-1}$)**

| | theory | | experiment | | | |
|---|---|---|---|---|---|---|
| | | rel intensities | ref 14 | ref 6 | | ref 2 |
| sym | scaled | IR | IR | Raman | IR | Raman |
| E | 186 | 0 | | 186(s) | | 178(s) |
| $A_2$ | 286 | 0 | | | | |
| E | 295 | 0 | | 300(m) | | 296(m) |
| E | 315 | 0 | | 313(w) | | 313(w) |
| $A_1$ | 337 | 0 | | 344(m) | | 344(m,p) |
| E | 413 | 3 | 415(m) | 415(m) | 417(m) | 415(m) |
| ? | | | | | | 451(w) |
| ? | | | | | | 466(w) |
| $A_1$ | 510 | 5 | | 505(s) | 502(w) | 505(s,p) |
| E | 562 | 0 | | missing | | |
| $A_1$ | 585 | 3 | | 592(s) | 598(m) | 592(s,p) |
| $A_1$ | 617 | 6 | 626(m) | 632(m) | 631(m) | 632(s,p) |
| E | 630 | 3 | 642(m) | 653(w) | 646(w) | 653(w) |
| $A_2$ | 659 | 0 | | | | |
| E | 687 | 2 | 663(m) | | 668(w) | |
| $A_1$ | 697 | 0 | 687(m) | 690(w) | 688(m) | 690(w,p) |
| E | 702 | 0 | | missing | | |
| $A_1$ | 812 | 0 | 850(m) | 814(w) | 830(m) | 814(w) |
| $A_1$ | 947 | 100 | 940−986(s) | 958(w) | 948(s,br) | 945(w,p) |
| E | 960 | 59 | | | | |
| | $2 \times 510$ | | | | 1010 | |
| | $2 \times 585$ | | | | 1202 | |
| | $2 \times 617$ | | | | 1264 | |
| | ? | | | | 2853 | |
| | ? | | | | 2924 | |

**TABLE 3: Comparison of the Calculated Vibrational Spectra of $P_4O_6S_2$ with Experimental Data (in $cm^{-1}$)**

| | theory | | experiment ref 3 | |
|---|---|---|---|---|
| sym | scaled | rel intensities IR | IR | Raman |
| $A_1$ | 156 | 0 | | 159(vs,p) |
| $B_1$ | 186 | 0 | | |
| $A_2$ | 194 | 0 | | 187(vs) |
| $B_2$ | 213 | 0 | | 205(m) |
| $B_1$ | 298 | 0 | | 290(w) |
| $A_2$ | 303 | 0 | | 301(w) |
| $A_1$ | 307 | 0 | | |
| $A_2$ | 326 | 0 | | |
| $B_2$ | 337 | 0 | | |
| $B_2$ | 346 | 0 | | 343(m) |
| $A_1$ | 351 | 0 | | 357(s,p) |
| $B_1$ | 426 | 4 | 421(s) | 420(w) |
| $A_1$ | 501 | 3 | 502(s) | 504(vs,p) |
| $B_2$ | 539 | 3 | 524(s) | 525(vw) |
| $B_1$ | 571 | 0 | | |
| $A_1$ | 585 | 0 | | 583(w) |
| $B_2$ | 627 | 13 | 628(s) | 632(m) |
| $A_1$ | 665 | 3 | 651(m) | 652(vw) |
| $A_2$ | 686 | 0 | | |
| $B_1$ | 689 | 4 | 677(m) | |
| $A_1$ | 691 | 0 | | |
| $B_1$ | 704 | 0 | | |
| $B_2$ | 731 | 0 | 728(vw) | |
| $A_2$ | 739 | 0 | | |
| $A_1$ | 741 | 1 | 742(vw) | |
| $B_2$ | 772 | 0 | | |
| $A_1$ | 855 | 0 | 849(w) | 848(w) |
| $B_2$ | 965 | 100 | 960(vs,br) | |
| $A_1$ | 972 | 72 | | |
| $B_1$ | 975 | 81 | | |

nuclear displacements within the $PO_3$ and $S{=}PO_3$ subunits provides a clear picture of changes within the $P_4O_6S_4$ series because their first ($P_4O_6$) and last ($P_4O_6S_4$) members are built of four equivalent $PO_3$ and $S{=}PO_3$ subunits, respectively. Furthermore, we distinguish between so-called "cage modes", which are primarily connected to vibrations of $P_4O_6$ cage atoms, and modes which are dominated by the terminal $P^V{=}S$ vibration.

**TABLE 4: Comparison of the Calculated Vibrational Spectra of $P_4O_6S_3$ with Experimental Data (in $cm^{-1}$)**

| | theory | | experiment ref 6 | |
|---|---|---|---|---|
| sym | scaled | rel intensities IR | IR | Raman |
| E | 148 | 0 | | 146(vs) |
| $A_1$ | 160 | 0 | | 155(vs) |
| | | | | 163(m) |
| E | 202 | 0 | | 198(s) |
| $A_2$ | 220 | 0 | inactive | |
| E | 300 | 0 | | 308(w) |
| E | 333 | 0 | | 326(w) |
| E | 342 | 1 | | 349(s) |
| $A_2$ | 370 | 0 | inactive | |
| $A_1$ | 365 | 1 | | 372(s) |
| | | | 450(vw) | 446(m) |
| $A_1$ | 479 | 4 | 486(s) | 485(vs) |
| E | 557 | 2 | 536(s) | |
| $A_1$ | 574 | 0 | 568(vw) | 568(w) |
| E | 642 | 13 | 639(vs) | 638(w) |
| | | 0 | 652(vw) | 656(vw) |
| $A_1$ | 673 | 1 | 666(vw) | 678(m) |
| E | 716 | 0 | 702(w) | 703(vw) |
| $A_1$ | 724 | 3 | 713(w) | 715(vw) |
| | | | 722(w) | |
| E | 744 | 1 | 767(m) | |
| $A_2$ | 774 | 0 | inactive | |
| E | 795 | 0 | missing | |
| $A_1$ | 891 | 3 | 894(sh) | 893(w) |
| $A_1$ | 970 | 67 | 960(vs,br) | |
| E | 974 | 100 | | 951(vw) |

**TABLE 5: Comparison of the Calculated Vibrational Spectra of $P_4O_6S_4$ with Experimental Data (in $cm^{-1}$)**

| theory | | | experiment | | | | | |
|---|---|---|---|---|---|---|---|---|
| | | | ref 1 | | ref 7 | | ref 8 | |
| sym | scaled | intensities IR | IR | Raman | IR | Raman | Raman | sym |
| | | | | | | | 95 | |
| | | | | 133(w) | | | | |
| E | 141 | 0 | | 145(vs) | | 148 | 150(dp) | E |
| | | | | 155(vs) | | | | |
| $F_2$ | 158 | 0 | | 160(vs) | | | | |
| | | | | 170(w) | | | | |
| | | | | | | 194 | 194(dp) | $F_2$ |
| $F_1$ | 220 | 0 | | | inactive | | | |
| | | | | | | 259 | | E |
| | | | | 271(vw) | | | | |
| | | | | 288(vw) | | | | |
| E | 315 | 0 | | 317(vw) | | | | |
| | | | | 328(w) | | | | |
| $F_2$ | 350 | 1 | | 352(m) | | 353 | 354(dp) | $F_2$ |
| $F_1$ | 365 | 0 | | | inactive | | | |
| | | | | 387(m) | | | | |
| $A_1$ | 392 | 0 | | 406(vs) | | 400 | 400(dp) | $A_1$ |
| | | | | 447(vw) | | | 447(p) | |
| | | | | | 460 | | | $F_2$ |
| | | | | | | | 498(dp) | |
| $F_2$ | 573 | 2 | | 548(m) | | | | |
| | | | | 569(m) | | | | |
| | | | 646(m) | 646(vw) | | | | |
| $F_2$ | 675 | 13 | 671(s) | 669(w) | | 666 | 668(dp) | $F_2$ |
| $A_1$ | 706 | 0 | 704(w) | 698(w) | | 694 | 700(dp) | $A_1$ |
| | | | 712(w) | 713(vw) | | | | |
| E | 744 | 0 | 753(w) | | 769 | | | $F_2$ |
| $F_1$ | 775 | 0 | | | inactive | | | |
| $F_2$ | 807 | 0 | | | missing | | | |
| | | | 882(m) | 898(vw) | | 897 | | E |
| $A_1$ | 929 | 0 | | 929(w) | | 930 | 934(p) | $A_1$ |
| $F_2$ | 986 | 100 | 978(vs) | | 981 | | | $F_2$ |
| | ? | | 1139(w) | | | | | |
| | ? | | 1214(m) | | | | | |
| | ? | | 1328(m) | | | | | |
| | ? | | 1388(m) | | | | | |

Couplings between cage vibrations and $P^V{=}S$ vibrations have to be considered to extract information about changes in the

**TABLE 6: Comparison of the Vibrational Spectra (in $cm^{-1}$)**

| modes description | $P_4O_6$ | $P_4O_6S$ | $P_4O_6S_2$ | $P_4O_6S_3$ | $P_4O_6S_4$ |
|---|---|---|---|---|---|
| linear combination of $P^V$═S bending vibrations | | 1 e 186 | 1 $a_1$ 156<br>1 $a_2$ 194 | 1 e 148<br>1 $a_1$ 160 | 1 e 141<br>1 $f_2$ 158 |
| bending vibration of $P^V$═S with contributions from the libration motion (see Figure 2) | | | 1 $b_1$ 186<br>1 $b_2$ 213 | 2 e 202<br>1 $a_2$ 365 | 1 $f_1$ 220 |
| symmetric bending of P−O−P cage bonds | 1 e 298 | 2 e 295 | 2 $a_1$ 307<br>2 $a_2$ 303 | 3 e 300 | 2 e 315 |
| umbrella motion of $PO_3$, respectively, S═$P^VO_3$ units (see Figure 2) | 1 $f_2$ 410 | 1 $a_1$ 337<br>3 e 315 | 3 $a_1$ 351<br>2 $b_2$ 337<br>2 $b_1$ 298 | 5 e 342<br>2 $a_1$ 220 | 2 $f_2$ 350 |
| libration motion of $PO_3$, respectively, S═$P^VO_3$ units (see Figure 2) | 1 $f_1$ 302 | 1 $a_2$ 286<br>4 e 413 | 3 $b_1$ 426<br>3 $a_2$ 326<br>3 $b_2$ 346 | 4 e 333<br>2 $a_2$ 370 | 2 $f_1$ 365 |
| cage breathing mode | 1 $a_1$ 597 | 3 $a_1$ 585 | 5 $a_1$ 501 | 3 $a_1$ 479 | 1 $a_1$ 392 |
| symmetric bending motion of O−$P^V$−O cage bond (see Figure 2 | 2 $f_2$ 570 | 2 $a_1$ 510<br>5 e 562 | 4 $a_1$ 585<br>4 $b_2$ 539<br>4 $b_1$ 571 | 6 e 557<br>4 $a_1$ 574 | 3 $f_2$ 573 |
| stretch motion (see Figure 2) | 3 $f_2$ 626 | 4 $a_1$ 617<br>6 e 630 | 6 $a_1$ 665<br>5 $b_2$ 627<br>5 $b_1$ 689 | 7 e 642<br>5 $a_1$ 673 | 4 $f_2$ 675 |
| umbrella mode (see Figure 2) | 2 $a_1$ 739 | 5 $a_1$ 697 | 7 $a_1$ 691 | 6 $a_1$ 724 | 2 $a_1$ 706 |
| antisymmetric stretching of $PO_3$ and S═$P^VO_3$ units, respectively (see Figure 2) | 2 e 633 | 7 e 687 | 8 $a_1$ 741<br>4 $a_2$ 686 | 8 e 716 | 3 e 730 |
| similar to the 2 e mode of $P_4O_6$ (see Figure 2) | 2 $f_1$ 645 | 2 $a_2$ 659<br>8 e 702 | 6 $b_1$ 704<br>5 $a_2$ 739<br>6 $b_2$ 731 | 9 e 744<br>3 $a_2$ 774 | 3 $f_1$ 775 |
| symmetric stretch ($\nu_s$) in $PO_3$ and S═$PO_3$ units, respectively (see Figure 2) | 4 $f_2$ 946 | 7 $a_1$ 947<br>9 e 960 | 9 $a_1$ 972<br>7 $b_2$ 965<br>7 $b_1$ 975 | 11 e 970<br>8 $a_1$ 974 | 6 $f_2$ 986 |
| neg. linear combination of stretching of $P^V$═S | | | 8 $b_2$ 772 | 10e 795 | 5 $f_2$ 807 |
| pos. linear combination of stretching of $P^V$═S | | 6 $a_1$ 812 | 10 $a_1$ 855 | 7 $a_1$ 891 | 3 $a_1$ 929 |

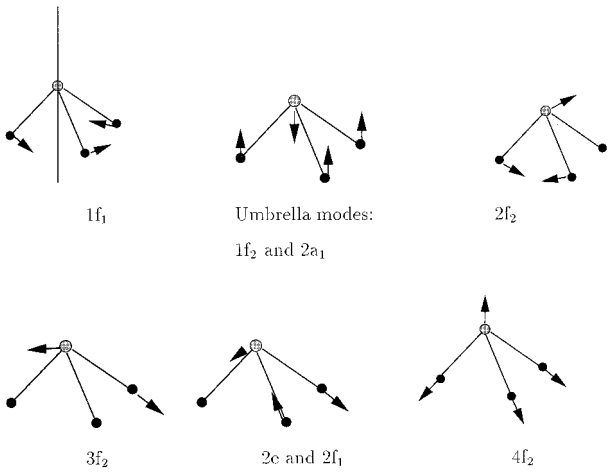


**Figure 2.** Pictorial representation of the vibrational modes of the P−$O_3$ unit of $P_4O_6$ cage structure.

bonding situation. Table 6 contains the correlation of the vibrational bands within the $P_4O_6S_m$ ($m = 0-4$) series and a brief description of the nuclear motions connected with each mode. The nuclear displacements of some modes are also indicated in Figure 2.

**a. Cage Modes.** In $P_4O_6$, the first cage mode appears at 298 $cm^{-1}$ (1e). It correlates with the 2e mode (295 $cm^{-1}$) of $P_4O_6S$, the 2$a_1$ (307 $cm^{-1}$), and 2$a_2$ (303 $cm^{-1}$) modes of $P_4O_6S_2$, the 3e mode (300 $cm^{-1}$) of $P_4O_6S_3$, and 2e (315 $cm^{-1}$) mode of $P_4O_6S_4$. These modes correspond to O−P−O bending vibrations of the $P_4O_6$ cage. Since the contributions from the $P^V$═S are negligible for these modes, the increase in the frequencies of these modes along the $P_4O_6S_m$ ($m = 0-4$) series is a first evidence for the reinforcement of the cage bonds within the $P_4O_6S_m$ ($m = 0-4$) series.

The next mode, within the $P_4O_6$ spectrum (1$f_2$: 410 $cm^{-1}$) represents a linear combination of umbrella motions of $PO_3$ subunits (Figure 2). It is related to the 2$f_2$ mode of $P_4O_6S_4$, which appears at 350 $cm^{-1}$. In this mode, $P^V$═S moves as a unit, i.e., the $P^V$═S distance is kept constant during the vibration. Consequently, the mass of the moving atoms increases along the $P_4O_6S_m$ ($m = 0-4$) series, resulting in a negative shift of the frequency along the series. The strongest frequency shift ($\approx$ 200 $cm^{-1}$)in the series is found for the cage breathing mode ($P_4O_6$: 1$a_1$ at 597 $cm^{-1}$; $P_4O_6S_4$: 1 $a_1$ at 392 $cm^{-1}$). Since the $P^{III}$ centers in the series are successively substituted by $P^V$═S groups, the shift again results from an increase of the mass of the moving atoms. For both modes, the $PO_3$ umbrella mode and the cage breathing mode, influences from the strengthening of the P−O cage bonds are small because they are mainly described by a cage bending motions in which the bond distances of the P−O cage bonds remains nearly constant.

The 2$f_2$ mode at 570 $cm^{-1}$ for $P_4O_6$ represents a symmetric bending motion of O−P−O cage bonds (Figure 2). It correlates to the 3$f_2$ mode of $P_4O_6S_4$. Both appear at the similar frequencies ($\approx$570 $cm^{-1}$). The small shift found for this mode results from a cancellation of the strengthening of the P−O cage bonds and the increase of the mass due to the substitution.

Modes involving the stretch motions of the P−O cage bond show a shift to higher frequency along the $P_4O_6S_m$ ($m = 0-4$) series. For $P_4O_6$, these modes occur at 626 $cm^{-1}$ (3$f_2$), 633 $cm^{-1}$ (2e), and 645 $cm^{-1}$ (2$f_1$). They are related to those modes of $P_4O_6S_4$ that appear at 675 $cm^{-1}$ (4$f_2$), 730 $cm^{-1}$ (3e), and 775 $cm^{-1}$ (3$f_1$). These modes represent linear combination of antisymmetric stretching vibrations of the P−O cage bonds (Figure 2). The increase of the frequencies (49, 97, 130 $cm^{-1}$, respectively) shows the increase in the bond strength of the cage bonds; the variation within the frequency shift results from the interplay between the **G** and **F** matrix elements.

For the $P_4O_6$, the highest cage mode appears at 946 $cm^{-1}$. It involves the symmetric stretch of the $PO_3$ unit (Figure 2). It can be related to the 6$f_2$ in the $P_4O_6S_4$ (986 $cm^{-1}$), but this mode possesses strong contribution from $P^V$═S vibrations.

Therefore, a detailed discussion about this mode will be provided in the next section.

**b. Vibrational Modes Involving the $P^V$=S Motions.** The modes which involve the bending of the $P^V$=S bond lie at the lower frequency range of the spectra (140−190 $cm^{-1}$), while the $P^V$=S stretching vibrations appear in the same energy region of the spectra as the cage stretching modes (900−1100 $cm^{-1}$).

Going from $P_4O_6S$ to multiple substituted compounds, the normal modes connected with the $P^V$=S stretch vibrations split into a mode representing the in-phase linear combination of the $P^V$=S stretch motions ($a_1$ symmetry) and one additional mode representing the out-of-phase linear combinations. The latter possesses $b_2$ symmetry (772 $cm^{-1}$) for $P_4O_6S_2$, e symmetry (795 $cm^{-1}$) for $P_4O_6S_3$, and $f_2$ symmetry (807 $cm^{-1}$) for $P_4O_6S_4$. The $a_1$ mode lies always at a higher frequency ($P_4O_6S_2$:10$a_1$, 855 $cm^{-1}$; $P_4O_6S_3$: 7$a_1$, 891 $cm^{-1}$; $P_4O_6S_4$: 3$a_1$, 929 $cm^{-1}$) than the out-of-phase modes.

The energetical ordering of the in-phase and out-of-phase mode is best understood in terms of two coupled $P^V$=S oscillators in a linear arrangement. In this model, the in-phase (symmetric) stretch mode ($S_1$) interacts with the vibration of both $P^V$ with respect to each other ($S_2$), while due to the symmetry, the out-of-phase (antisymmetric) stretch mode ($S_3$) cannot couple. When both terminal $P^V$=S oscillators are not coupled ($F_{21} = 0$), clearly the modes connected with the $S_1$ and $S_3$ are degenerate and, in this case, the frequency of the $S_2$ mode is zero. For $F_{22} > 0$ (i.e., increasing coupling), the frequency associated with the vibration of both $P^V$=X units with respect to each other ($S_2$) becomes greater than zero and due to its coupling with the $S_1$ vibration, shifts the frequency of this vibration to higher frequencies, while the frequency of the out-of-phase stretch mode remains unchanged. The splitting between the in-phase and the out-of-phase combination increases from about 80 $cm^{-1}$ for $P_4O_6S_2$ to about 120 $cm^{-1}$ for $P_4O_6S_4$. This splitting increases because the frequency shift found within the $P_4O_6S_4$ series is more pronounced for the in-phase combination than for the out-of-phase combination (117 $cm^{-1}$ vs 35 $cm^{-1}$). For $P_4O_6S_4$, couplings between cage and $P^V$=S vibrations are furthermore found in the 5$f_2$ mode (807 $cm^{-1}$) and the 6$f_2$ (986 $cm^{-1}$) mode. While the former corresponds mainly to an out-of-phase stretching motion of the $P^V$=S, with a small contribution of cage vibration, the 6$f_2$ can be described as a cage mode with a small contribution of the $P^V$=S out-of-phase stretching.

The lower frequency range of the spectra (<250 $cm^{-1}$) involves only bending vibrations of the $P^V$=S units. For $P_4O_6S_2$, four modes result from the linear combination of the two terminal $P^V$=S bending motion: $a_1$ (156 $cm^{-1}$), $b_2$ (213 $cm^{-1}$), $a_2$ (194 $cm^{-1}$), $b_1$ (186 $cm^{-1}$). While the $a_1$ ($b_2$) mode represents mainly the negative (positive) linear combination of the $P^V$=S bending motion within the mirror plane cutting through both S atoms (Figure 1), the $a_2$ mode (negative linear combination) and $b_1$ mode (positive linear combination) are built from the $P^V$=S bending vibrations perpendicular to this mirror plane. Going from $P_4O_6S_2$ to $P_4O_6S_3$, the modes $a_1$ and $a_2$ transform into the 1e mode, which is at 148 $cm^{-1}$ for the $P_4O_6S_3$, and correlates to the 1e (141 $cm^{-1}$) mode in the $P_4O_6S_4$ spectrum.

Comparing the nuclear vibrations for $P_4O_6$ and for $P_4O_6S_4$, one notices that both modes 1$f_1$ (220 $cm^{-1}$) and 2$f_2$ of $P_4O_6S_4$ (350 $cm^{-1}$) are related to the 1$f_1$ mode (302 $cm^{-1}$) of the $P_4O_6$. Both can be described as combinations of the libration motion of $PO_3$ units with the terminal $P^V$=S bending motions (Figure 2). The contribution of the $P^V$=S bending vibrations is responsible for the low frequency of the 1$f_1$ mode of $P_4O_6S_4$ (220 $cm^{-1}$). On the other hand, the higher frequency of the 2$f_1$ mode of $P_4O_6S_4$ lying about 60 $cm^{-1}$ above the 1$f_2$ of $P_4O_6$ results from O−P−O bending motions of the cage. For $P_4O_6S$, $P_4O_6S_2$, and $P_4O_6S_3$, contributions of the $PO_3$ libration are found in almost all $P^V$=S bending modes. The increased coupling results from the lower symmetry of these molecules.

**Comparison between $P_4O_6S_m$ ($m = 0-4$) and $P_4O_n$ ($n = 6-10$) series.** Comparing both series, the strongest differences can be expected for modes involving the terminal bond $P^V$=S or $P^V$=O. In both series the bending motion of $P^V$=X represents the energetically lowest bands. Going from oxygen to sulfur substituents, the frequency of the $P^V$=X bending decreases by about 110 $cm^{-1}$. This shift results from differences in the mass (16 amu) and the bond distance (0.4 Å).

The strong decrease of the $P^V$=X stretching mode, if X = O is compared to X = S, is obviously related to the decrease in the $P^V$=S bond strength. While the $P^V$=S stretching motions appear in the same energy region as the stretching vibration of the $P_4O_6$ cage (900 $cm^{-1}$), the $P^V$=O stretch modes lie much higher (1300 $cm^{-1}$). This indicates that the product of the **G** and **F** matrix elements connected with $P^V$=S bond stretching motion is similar to that connected with P−O cage bonds stretching, while for $P^V$=O bonds this product is much higher.

The different splitting between the in-phase and the out-of-phase linear combinations of the $P^V$=X stretching motions (e.g. $P_4O_8$: 18 $cm^{-1}$, $P_4O_6S_2$: 83 $cm^{-1}$) results from differences in the bond-strength of the P=X bond and the different masses.

Differences in the cage modes are more interesting than the obvious effects in the $P^V$=X motions discussed above. Within both series, the cage breathing modes possess the strongest shift to lower frequencies ($P_4O_6S_m$: 205 $cm^{-1}$; $P_4O_n$: 68 $cm^{-1}$). The difference between both series results from the greater increase in the reduced mass, when the $P^{III}$ unit is replaced by the $P^V$=S and the $P^V$=O unit, respectively.

In both series, strong positive frequency shifts are found for those modes connected with the 3$f_2$ (626 $cm^{-1}$), the 2e (633 $cm^{-1}$), and the 2$f_1$ (645 $cm^{-1}$) mode of $P_4O_6$. These modes correlate with the 4$f_2$, the 3e, and the 3$f_1$, respectively, in the $P_4O_6X_4$ spectrum (X = O, S) (Table 6 and ref 4). For $P_4O_n$ ($n = 6-10$), we find frequency shifts of 141, 178, and 187 $cm^{-1}$, respectively, while 49, 97, and 130 $cm^{-1}$, respectively are obtained for the $P_4O_6S_m$ ($m = 0-4$) series. This shows that the shifts increase by a factor of 3 for the first and a factor of 1.5−1.8 for the two others, if one goes from the $P_4O_n$ ($n = 6-10$) to the $P_4O_6S_m$ ($m = 0-4$) series. The large difference in the shift of the first mode (4$f_2$) results from coupling between cage vibrations and $P^V$=X stretch vibrations. Such coupling occurs only for $P_4O_6S_m$ ($m = 0-4$) series. For the 3e and the 3$f_1$ modes, the couplings between cage and $P^V$=X vibrations are smaller. Therefore, the different frequency shifts in these two cage modes comparing the $P_4O_n$ ($n = 6-10$) and the $P_4O_4S_m$ ($m = 0-4$) series indicate a somewhat larger increase in the P−O cage bonding strength in the oxygen-substituted compounds relative to the sulfur substitution. This finding is also reflected the computed force constants. As expected, in going from $P_4O_6S_2$ to $P_4O_8$, this constant increases from 0.484 to 0.518 au for the $P^V-O_c$ stretch motion, and from 0.417 au to 0.445 au for $P^V-O_b$ stretching, while those related to $P^{III}-O_a$ stretching are virtually identical in both compounds (0.366 vs 0.367 au).

Such interpretation that the P−O cage bond of the oxygen-substituted compounds is somewhat stronger than those of the sulfur-substituted compounds is also supported by comparing the P−O bond lengths in the cage in going from $P_4O_6$ to $P_4O_{10}$.

**Acknowledgment.** The authors thank Dr. Miljenko Perić for fruitful discussions. This work was supported by the Deutsche Forschungsgemeinschaft (Sonderforschungsbereich 334).

## References and Notes

(1) Clade, J.; Frick, F.; Jansen, M. *Adv. Inorg. Chem.* **1994**, *41*, 327.

(2) Valentim, A. R. S.; Engels, B.; Peyerimhoff, S. D.; Clade, J.; Jansen, M. *Inorg. Chem.* **1997**, *36*, 2451.

(3) Valentim, A. R. S.; Engels, B.; Peyerimhoff, S. D.; Tellenbach, A.; Strojek, S.; Jansen, M. *Z. Anorg. Allg. Chem.* **1998**, *624*, 642.

(4) Valentim, A. R. S.; Engels, B.; Peyerimhoff, S. D.; Clade, J.; Jansen, M. *J. Phys. Chem. A* **1998**, *21*, 3690.

(5) Pulay, P.; Forgarasi, G.; Ponger, G.; Boggs, J. E.; Vargha, A. *J. Am. Chem. Soc.* **1983**, *105*, 7037.

(6) Frick, F. Dissertation, Bonn University, 1993.

(7) Zijp, D. H. *Adv. Mol. Spectrosc.* **1962**, *1−3*, 345.

(8) Gerding, H.; v. Bredemode, H. *Recl. Trav. Chim. Pays-Bas* **1945**, *64*, 549.

(9) Huzinaga, H. *Approximate Atomic Wave functions, I, II*. Department of Chemistry Report, University of Alberta, Alberta, Canada, 1965.

(10) Frisch, M. J.; Trucks, G. W.; Schlegel, H. B.; Gill, P. M. W.; Johnson, B. G.; Robb, M. A.; Cheeseman, J. R.; Keith, T.; Petersson, G. A.; Montgomery, J. A.; Raghavachari, K.; Al-Laham, M. A.; Zakrzewski, V. G.; Ortiz, J. V.; Foresman, J. B.; Cioslowski, J.; Stefanov, B. B.; Nanayakkara, A.; Challacombe, M.; Peng, C. P.; Ayala, P. Y.; Chen, W.; Wong, M. W.; Andres, J. L.; Reploge, E. S.; Gomperts, R.; Martin, R. L.; Fox, J. F.; Bincley, J. S.; DeFrees, D. J.; Baker, J.; Stewart, J. J. P.; Pople, J. A. *Gaussian94*; Killedan Inc.: Pittsburgh, PA, 1995.

(11) Pulay, P., and co-workers, TX90, Fayetteville, AR, 1990.

(12) Schafternaar, G., MOLDEN, CAOS/CAMM Center Nijmegen, Toernooiveld, Nijmegen, The Netherlands, 1991.

(13) Mühlhäuser, M.; Engels, M.; Marian, C. M.; Peyerimhoff, S. D.; Bruna, P. B.; Jansen, M. *Angew. Chem.* **1994**, *106*, 576.

(14) Walker, M. L.; Peckenpaugh, D. E.; Mills, J. L. *Inorg. Chem.* **1979**, *18*, 2792.

(15) Wilson, E. B.; Decius, J. C.; Cross, P. C. *Molecular Vibrations*; McGraw-Hill: New York, 1955.